



Published in final edited form as:

*Circ Res.* 2019 April 26; 124(9): 1360–1371. doi:10.1161/CIRCRESAHA.118.314607.

## Mitophagy Is Essential for Maintaining Cardiac Function During High Fat Diet-Induced Diabetic Cardiomyopathy

Mingming Tong, Toshiro Saito, Peiyong Zhai, Shin-ichi Oka, Wataru Mizushima, Michinari Nakamura, Shohei Ikeda, Akihiro Shirakabe, and Junichi Sadoshima

Department of Cell Biology and Molecular Medicine, Rutgers-New Jersey Medical School, USA

### Abstract

**Rationale:** Diabetic patients develop cardiomyopathy characterized by hypertrophy, diastolic dysfunction, and intracellular lipid accumulation, termed lipotoxicity. Diabetic hearts utilize fatty acids as a major energy source, which produces high levels of oxidative stress, thereby inducing mitochondrial dysfunction.

**Objective:** To elucidate how mitochondrial function is regulated in diabetic cardiomyopathy.

**Methods and Results:** Mice were fed either a normal diet (ND) or high fat diet (HFD, 60 kcal % fat). Although autophagic flux was activated by HFD consumption, peaking at 6 weeks ( $p < 0.05$ ), it was attenuated thereafter. Mitophagy, evaluated with Mito-Keima, was increased after 3 weeks of HFD feeding (mitophagy area: 8.3% per cell with ND and 12.4% with HFD) and continued to increase even after 2 months ( $p < 0.05$ ). By isolating adult cardiomyocytes from GFP-LC3 mice fed HFD, we confirmed that mitochondria were sequestered by LC3 positive autophagosomes during mitophagy. In wild type (WT) mice, cardiac hypertrophy, diastolic dysfunction (EDPVR =  $0.051 \pm 0.009$  in ND and  $0.11 \pm 0.004$  in HFD) and lipid accumulation occurred within 2 months of HFD feeding ( $p < 0.05$ ). Deletion of *atg7* impaired mitophagy, increased lipid accumulation, exacerbated diastolic dysfunction (EDPVR =  $0.11 \pm 0.004$  in WT and  $0.152 \pm 0.019$  in *atg7* cKO,  $p < 0.05$ ) and induced systolic dysfunction (ESPVR =  $24.86 \pm 2.46$  in WT and  $15.93 \pm 1.76$  in *atg7* cKO,  $p < 0.05$ ) during HFD feeding. Deletion of Parkin partially inhibited mitophagy, increased lipid accumulation and exacerbated diastolic dysfunction (EDPVR =  $0.124 \pm 0.005$  in WT and  $0.176 \pm 0.018$  in Parkin KO,  $p < 0.05$ ) in response to HFD feeding. Injection of Tat-Beclin1 (TB1) activated mitophagy, attenuated mitochondrial dysfunction, decreased lipid accumulation, and protected against cardiac diastolic dysfunction (EDPVR =  $0.110 \pm 0.009$  in Control peptide and  $0.078 \pm 0.015$  in TB1,  $p < 0.05$ ) during HFD feeding.

**Conclusions:** Mitophagy serves as an essential quality control mechanism for mitochondria in the heart during HFD consumption. Impairment of mitophagy induces mitochondrial dysfunction and lipid accumulation, thereby exacerbating diabetic cardiomyopathy. Conversely, activation of mitophagy protects against HFD-induced diabetic cardiomyopathy.

**Address correspondence to:** Dr. Junichi Sadoshima, Department of Cell Biology and Molecular Medicine, Rutgers-New Jersey Medical School, 185 S Orange Ave, MSB G609, Newark, NJ 07103, sadoshju@njms.rutgers.edu.

DISCLOSURES

None.

## Keywords

High fat diet; mitophagy; autophagy; mitochondria; lipid accumulation; cardiac dysfunction; diabetic cardiomyopathy; lipotoxicity; Cell Biology/Structural Biology; Cell Signaling/Signal Transduction; Metabolism

---

## INTRODUCTION

The prevalence of obesity is increasing rapidly worldwide, with 107.7 million children (5.0% of all children) and 603.7 million adults (12.0% of all adults) reported as obese in 2015<sup>1</sup>. Cardiovascular disease has been the leading cause of death and disability-adjusted life years in patients with high body mass index (BMI)<sup>1</sup>. More than one third of diabetic patients develop myocardial dysfunction, known as diabetic cardiomyopathy<sup>2</sup>, even in the absence of conventional cardiac risk factors, such as coronary artery disease, hypertension, and valvular heart disease. In its early phase, left ventricular (LV) hypertrophy, fibrosis and diastolic dysfunction with normal ejection fraction are observed. Some patients develop heart failure with preserved ejection fraction (HFpEF), whereas others eventually develop heart failure with reduced ejection fraction (HFrEF)<sup>3,4</sup>.

The adult heart is a high energy-demanding tissue and 60%–90% of the energy used originates from fatty acid oxidation in mitochondria<sup>5</sup>. Diabetic hearts shift away from utilization of glucose, and depend almost completely on fatty acids as an energy source, which generally produces more oxidative stress during their oxidation and eventually causes mitochondrial dysfunction<sup>6</sup>. In addition, due to the imbalance between fatty acid uptake and fatty acid oxidation, accumulations of fatty acids called lipid droplets (LDs) often develop in the cytosol of cardiomyocytes (CMs) as well as in the vascular structure. Accumulation of some forms of fatty acids, including ceramide and diacylglycerol, exerts cytotoxicity, thereby inducing histological and functional disturbances in the heart, termed lipotoxicity<sup>7</sup>.

Macroautophagy is characterized by the presence of double-membrane vesicles, called autophagosomes, which contain cytosolic proteins and organelles and are degraded by lysosomal enzymes. When macroautophagy selectively degrades mitochondria, it is termed mitophagy<sup>5</sup>. Increasing lines of evidence suggest that mitophagy plays an important role in degrading damaged or unnecessary mitochondria in CMs at baseline and in response to stress<sup>8,9</sup>. Together with mitochondrial fission and fusion and mitochondrial biogenesis, mitophagy is one of the most important steps necessary to maintain the quality of mitochondria<sup>10</sup>. Diabetic cardiomyopathy is commonly accompanied by the presence of mitochondrial dysfunction. In fact, previous studies have shown that autophagy, which non-selectively degrades mitochondria, and mitophagy are either downregulated<sup>11,12,13,14,15</sup> or upregulated<sup>16,17</sup> in the heart with metabolic syndrome. Importantly, the occurrence of mitophagy in the heart during the development of diabetic cardiomyopathy and its underlying mechanism are not unequivocally documented. Furthermore, how stimulation or inhibition of mitophagy affects the development of diabetic cardiomyopathy has been poorly addressed. We believe that a better understanding of how mitophagy is regulated during diabetic cardiomyopathy is essential in order to develop a specific strategy to alleviate cardiac dysfunction in type II diabetic patients.

We therefore asked the following questions: 1) Is mitophagy activated during the development of diabetic cardiomyopathy and, if so, what is the underlying molecular mechanism stimulating mitophagy? 2) What is the role of mitophagy during the development of diabetic cardiomyopathy? We addressed these questions using recently developed mitophagy indicator mice and loss-of-function mouse models of autophagy and mitophagy.

## METHODS

The authors declare that all supporting data are available within the article (and its online supplementary files in the Online Data Supplement).

Detailed methods can be found in the Online Data Supplement.

## RESULTS

### **Autophagy is upregulated in the early phase but downregulated in the late phase of HFD consumption.**

We have shown previously that HFD consumption induces diastolic dysfunction, cardiac hypertrophy and insulin resistance in mice<sup>12</sup>. In order to evaluate the effect of HFD consumption on autophagy in the heart, C57BL/6J mice were fed with either normal diet (ND) or HFD for the indicated durations. Assessment of left ventricular (LV) diastolic function by pressure-volume loop (PV-Loop) analysis showed that HFD consumption significantly increases the end diastolic pressure-volume relationship (EDPVR) compared to ND consumption at 2 months and thereafter (Online Table I and Online Figure I), suggesting that HFD induces LV diastolic dysfunction within 2 months, consistent with our previous results<sup>12</sup>. In order to evaluate the role of autophagy and mitophagy during the initial development of diabetic cardiomyopathy, we focused on the initial phase, namely 0–2 months, in this study.

To assess autophagic flux, we treated mice with chloroquine (CQ)<sup>18</sup>, an inhibitor of fusion between autophagosomes and lysosomes, 4 hours before euthanasia, and quantified the level of LC3II. HFD feeding increased the level of LC3II, peaking at 6 weeks (Figure 1AB). HFD feeding also enhanced CQ-induced increases in LC3II, indicating increases in autophagic flux, peaking at 6 weeks. However, even in the presence of CQ, the LC3II level was the same as at baseline after 2 months of HFD consumption, suggesting that autophagic flux returns to the basal level by 2 months (Figure 1AB). The effect of HFD on cardiac autophagic flux was also evaluated in transgenic mice with CM-specific expression of tandem fluorescent mRFP-GFP-LC3 (Tf-LC3)<sup>18,19</sup>, in which autophagosomes emit both green (GFP) and red (mRFP) fluorescence, resulting in a yellow signal in merged images, whereas autolysosomes emit red (mRFP) fluorescence only. Tf-LC3 mice were fed with HFD for 6 weeks and 2 months, and then treated with CQ 4 hours before euthanasia. The number of yellow dots (autophagosomes) was significantly greater in mice fed with HFD than in those with ND. CQ significantly enhanced increases in yellow dots (autophagosomes) in mice fed with HFD for 6 weeks compared to in those with ND, suggesting that autophagic flux is increased after HFD feeding for 6 weeks. In contrast, CQ-

induced increases in yellow dots were attenuated in mice fed with HFD for 2 months compared to in those fed with ND (Figure 1CD), suggesting that autophagic flux was impaired at 2 months of HFD feeding. Taken together, these results indicate that although autophagic flux is activated by HFD consumption, peaking at 6 weeks, it is attenuated by 2 months of HFD consumption.

In order to elucidate the signaling mechanism by which autophagy is activated in response to HFD consumption, we evaluated the activity of known regulators of autophagy. We and others have shown previously that autophagy in the heart is negatively regulated by two major signaling pathways, namely mammalian sterile 20 like kinase 1 (Mst1)<sup>20</sup> and mTOR<sup>12</sup>. Thus, we investigated how HFD consumption affects these signaling mechanisms. HFD consumption led to inhibition of Mst1 whereas mTOR was not affected (online Figure IIA-C), suggesting that downregulation/inactivation of Mst1 may contribute to the initial activation of autophagy/mitophagy in response to HFD consumption. ULK1 was also activated after HFD feeding (online Figure IID). Thus, ULK1 may also contribute to activation of autophagy in response to HFD consumption.

### **Mitophagy was upregulated in response to HFD consumption.**

Organelle-specific autophagy, including mitophagy, plays an important role in maintaining cellular functions during stress. We thus investigated whether HFD-induced increases in autophagy are accompanied by increases in mitophagy. The level of mitophagy in CMs was evaluated using transgenic mice expressing Mito-Keima in a cardiac-specific manner (Tg-Mito-Keima). Mito-Keima fluorescence shows a shift in its excitation to higher wavelengths when mitochondria come into contact with the acidic milieu of lysosomes during mitophagy<sup>21</sup>. The ratio of Keima fluorescence at an excitation wavelength of 561 nm to that at 457 nm increases with a drop in pH, namely when mitophagy is activated. HFD feeding time-dependently increased the Mito-Keima-positive area in CMs, suggesting that mitophagy is activated by HFD feeding (Figure 2AB). The area of high 561/457 ratio dots was increased as early as at 3 weeks of HFD feeding and continued to increase even after 2 months. We also evaluated mtDNA/nuclear DNA, with real-time PCR of cytochrome b<sup>9</sup> and  $\beta$ -actin (Figure 2C). The mtDNA/nuclear DNA ratio was significantly smaller in CMs isolated from mice fed with HFD for 2 months than in those with ND, consistent with decreases in mitochondrial content. These results suggest that mitophagy is activated in the heart in response to HFD feeding.

In order to investigate how mitophagy is activated in response to HFD consumption, we isolated the mitochondrial fraction from the whole hearts after 2 months of either ND or HFD feeding. The level of LC3II was increased in response to HFD feeding in the total lysate and in the mitochondrial fraction, but not in the supernatant, primarily consisting of the cytosolic fraction. The level of LC3II was further increased in the presence of CQ in the mitochondrial fraction but not in the supernatant (Figure 2DE), suggesting that autophagy is activated predominantly in the mitochondrial fraction in CMs in response to HFD feeding. In order to confirm that mitochondria are sequestered by LC3 positive autophagosomes during mitophagy in response to HFD feeding, we investigated co-localization of mitochondria and LC3. To this end, GFP-LC3 transgenic mice<sup>12</sup> were subjected to ND or

HFD feeding. After 2 months, CMs were freshly isolated and subjected to staining with Mitotracker Red. Co-localization of GFP-LC3 (green) with Mitotracker (red) increased significantly more in CMs isolated from mice treated with HFD than in those with ND (Figure 2F-H). High magnification microscopic images showed that more than 75% of GFP-LC3 exhibited a ring-like structure with a diameter of 500 nm (Figure 2FG), and that around 75% of the LC3 ring-like structures surrounded Mitotracker red signals (Figure 2FH). These results suggest that LC3 positive autophagosomes sequester mitochondria in CMs in response to HFD feeding. Taken together, these results suggest that autophagy is activated primarily in the mitochondrial fraction and sequesters mitochondria into LC3-positive autophagosomes.

### **Autophagy and mitophagy induced by HFD feeding are attenuated in *atg7* cKO mice.**

In order to elucidate the role of mitophagy in the regulation of cardiac lipid metabolism, we used cardiac specific *atg7* knock-out (*atg7* cKO) mice. *Atg7* cKO mice were fed HFD for two months. Expression of LC3II was reduced due to a decrease in LC3I processing in the hearts of *atg7* cKO mice in both the presence and absence of HFD feeding, suggesting that general autophagy is completely suppressed in *atg7* cKO mice (Figure 3A). In order to evaluate whether mitophagy is impaired in *atg7* cKO mice we crossed *atg7* cKO or WT mice with Tg-Mito-Keima. The area of high 561/457 ratio dots was significantly smaller in *atg7* cKO mice than in WT mice fed with either ND or HFD, suggesting that *Atg7* plays an essential role in mediating mitophagy at baseline and in response to HFD feeding (Figure 3BC). Consistently, the mitochondrial DNA content was greater in *atg7* cKO mice fed with HFD than in control mice (Figure 3D).

### **Atg7-dependent autophagy protects the heart during HFD consumption.**

We then investigated the functional significance of autophagy and mitophagy during HFD consumption. To this end, control and *atg7* cKO mice were subjected to either ND or HFD feeding for 2 months and the extent of cardiac hypertrophy and cardiac function were evaluated. Whereas HFD feeding significantly increased the LV weight/tibia length ratio (LVW/TL) in control mice, it further increased LVW/TL in *atg7* cKO mice (Figure 3E). Although HFD feeding did not significantly affect left ventricular ejection fraction (LVEF) in control mice as evaluated with echocardiographic analyses, it significantly reduced LVEF in *atg7* cKO mice (Figure 3FG and Online Table II). PV-Loop analyses indicated that HFD feeding significantly reduced the end systolic pressure-volume relationship (ESPVR) in *atg7* cKO, but not in control mice (Figure 3H and Online Table III), consistent with the aforementioned echocardiography result that HFD feeding induces systolic dysfunction in *atg7* cKO mice. HFD feeding induced-increases in the slope of the end diastolic pressure-volume relationship (EDPVR) observed in control mice were further increased in *atg7* cKO (Figure 3I and Online Table III). These results suggested that *Atg7* protects the heart against cardiac hypertrophy and both systolic and diastolic dysfunction during HFD consumption.

### **Mitochondrial dysfunction is exacerbated in *atg7* cKO mice.**

Since the impairment of mitophagy in *atg7* cKO mice may affect mitochondrial quality control mechanisms, we evaluated mitochondrial function. To this end, we used isolated adult CMs to evaluate mitochondrial membrane potential (MMP) with TMRE incubation

and perform flow cytometric analyses, as well as confocal microscopy. Although HFD feeding for 2 months significantly reduced the MMP in CMs isolated from control mice, it further reduced the MMP in CMs from *atg7* cKO mice (Figure 3J and Online Figure IIIAB). Whereas the oxygen consumption rate (OCR), evaluated with a Seahorse XF96 analyzer, was decreased by HFD feeding in CMs isolated from control mice, it was further reduced in those from *atg7* cKO mice (Figure 3K). Fatty acid oxidation was increased by HFD feeding in CMs isolated from control mice, but not from *atg7* cKO mice, compared to in CMs isolated from control mice fed with ND (Figure 3L). These results suggested that downregulation of autophagy and mitophagy induces accumulation of dysfunctional mitochondria during HFD consumption.

### **Lipid accumulation, fibrosis and cell death are enhanced in *atg7* cKO mice compared to in WT mice in response to HFD.**

EM analysis of myocardial sections in control mice showed that HFD feeding for 2 months significantly increased vacuolar spaces adjacent to mitochondria, most likely LDs, in control mice. The LDs were greater in *atg7* cKO mice fed with HFD than in WT mice with HFD (Figure 4AB). LDs are located next to mitochondria and appear to have physical contact with mitochondria (Figure 4C). The myocardial triglyceride content was increased significantly in control mice fed with HFD, and it was further increased in *atg7* cKO mice fed with HFD (Figure 4D). Oil red O staining also indicated that myocardial accumulation of lipid was significantly increased by HFD feeding in control mouse hearts and it was further enhanced in *atg7* cKO mice (Figure 4EF).

Lipophagy is a lipid-specific form of autophagy involved in the transfer of lipid from LDs to lysosomes wherein lipolysis takes place and fatty acids are released into the cytoplasm<sup>22</sup>. We investigated whether lipophagy is induced by HFD feeding in the heart. Despite extensive examination of myocardial sections with EM, however, we were not able to identify double membrane structures containing lipids in control mice with HFD feeding. Similarly, we could not find co-localization of GFP-LC3 ring-like structure or dots with lipids in CMs freshly isolated from control mice subjected to HFD feeding (Figure 4G), although we could observe co-localization of GFP-LC3 with lipids in CMs freshly isolated from mice with starvation condition (Online Figure IV). These results suggest that lipophagy may not be activated at significant levels in the mouse heart in the presence of HFD feeding.

HFD feeding significantly increased cardiac fibrosis, as evaluated with Picrosirius red (PSR) staining, in *atg7* cKO mice, but not in control mice (Online Figure VAB). HFD also significantly increased the number of TUNEL positive CMs and the myocardial level of cleaved Caspase 3 in *atg7* cKO mice but not in control mice (Online Figure VC-F). Taken together, these data indicated that Atg7 protects the heart against CM fibrosis and apoptosis during HFD consumption.

### **Parkin-mediated mitophagy protects the heart against HFD-induced cardiac hypertrophy, diastolic dysfunction and lipid accumulation.**

Mitophagy is mediated at least in part through Parkin-dependent mechanisms in the heart<sup>5</sup>. Parkin protein was increased in the whole cell and in mitochondrial fractions during HFD



consumption compared to ND consumption (online Figure VI A-C). We crossed Parkin KO mice with Tg-Mito-Keima. The HFD-induced increase in the area of high 561/457 ratio dots was significantly smaller in Parkin KO mice (Figure 5AB). Although HFD consumption increased the level of ubiquitinated proteins in the mitochondrial fraction in control mice compared to ND consumption, the HFD-induced increase in ubiquitinated proteins in the mitochondrial fraction was significantly attenuated in Parkin KO mice (online Figure VI A and D). Parkin KO mice developed more severe cardiac hypertrophy and cardiac diastolic dysfunction as evaluated with PV-Loop analyses, in response to HFD feeding (Figure 5CD, Online Table IV). Systolic function, evaluated by echocardiographic measurement was maintained in both control and Parkin KO mice (Online Table V). Compared with WT mice fed HFD, Parkin KO mice fed HFD exhibited decreased MMP and fatty acid oxidation (Figure 5EF). These results suggest that downregulation of mitophagy during HFD consumption induces accumulation of dysfunctional mitochondria. The HFD-induced decreases in MMP observed in WT mice were exacerbated in Parkin KO mice. HFD feeding significantly increased fatty acid oxidation in control mice but not in Parkin KO mice.

EM analysis showed that the LDs induced by HFD feeding are significantly larger in Parkin KO mice than in control mice (Figure 5GH). The myocardial triglyceride content was significantly greater in Parkin KO mice with HFD than in control mice fed with HFD (Figure 5I). Oil red O staining indicated that myocardial accumulation of lipid in response to HFD feeding was significantly greater in Parkin KO mice than in control mice (Figure 5JK). It should be noted that the size of LDs and the extent of Triglyceride accumulation observed in Parkin KO mice fed with HFD were not as great as those in *atg7*cKO mice fed with HFD.

Taken together, these observations show that downregulation of Parkin impairs mitophagy and partially mimics the cardiac phenotype in *atg7*cKO mice in response to HFD consumption. These results suggest that Atg7- and Parkin-induced mitophagy plays an important role in protecting the heart during HFD consumption.

#### **HFD-induced cardiac dysfunction is attenuated by TAT-Beclin 1 treatment.**

Since downregulation of autophagy and mitophagy induces cardiac hypertrophy and dysfunction in response to HFD consumption, we next investigated whether stimulation of autophagy and mitophagy alleviates cardiac hypertrophy and LV dysfunction induced by HFD consumption. We have shown previously that intraperitoneal injection of TAT-Beclin1 (TB1)<sup>23</sup> increases mitophagy in the heart<sup>9</sup>. TB1 contains 18 amino acids derived from Beclin1 (267–284) and potently stimulates autophagy in HeLa and other cells by mobilizing endogenous Beclin1 from the Golgi apparatus where Beclin1 is tethered through Golgi-associated plant pathogenesis-related protein 1<sup>23</sup>. We injected TB1 or control TAT-scramble (TS) into mice during the last 2 weeks of HFD feeding. TB1 treatment significantly increased LC3II in total and mitochondrial fractions compared to TS treatment in the presence of both ND and HFD consumption (online Figure VII A and B). Importantly, the level of LC3II was greater in the mitochondrial fraction than in the supernatant fraction, suggesting that TB1-activated autophagy primarily targets mitochondria during HFD consumption. After 3 months of HFD feeding, HFD-induced increases in mitophagy, as evaluated with Tg-Mito-Keima, were significantly greater in TB1-injected mice than in TS-

injected mice (Figure 6AB). HFD feeding-induced cardiac diastolic dysfunction was significantly attenuated in TB1 treated mice compared to in TS treated mice (Figure 6C and Online Table VI). Mitochondrial function was evaluated using isolated adult CMs. Although HFD feeding significantly decreased the OCR in TS treated mice, TB1 treatment significantly attenuated the HFD-induced decrease in the OCR (Figure 6D). TB1 treatment also blunted HFD-induced depolarization of the MMP, as evaluated with TMRE (Figure 6EF). Oil red O staining of cardiac tissues indicated that HFD-induced increases in lipid accumulation were significantly attenuated by TB1 compared to TS (Figure 6GH). These results suggest that TB1 treatment attenuates HFD-induced mitochondrial dysfunction, myocardial accumulation of lipid, and cardiac diastolic dysfunction, at least in part through improvement of mitophagy.

We next tested whether TB1 rescues impaired mitophagy and cardiac dysfunction during HFD consumption in Parkin KO mice. We crossed Parkin KO with Mito-Keima mice and injected them with TB1. TB1 restored mitophagy and rescued LV diastolic dysfunction (online figure VIII A-C). These results suggest that TB1 activates mitophagy even in the absence of Parkin during HFD consumption, and that Parkin-independent mitophagy is also effective in improving cardiac dysfunction induced by HFD consumption.

We next assessed whether stimulation of mitophagy during HFD consumption leads to improvement in the overall quality of mitochondria. First, we evaluated whether transcription factors involved in mitochondrial biogenesis are upregulated by TB1 injection during HFD consumption. Although PGC1 $\alpha$  and Tfam did not change, NRF1 was significantly upregulated in response to TB1 injection in the presence of either ND or HFD consumption (online Figure IX A and B), indicating that mitochondrial biogenesis may be activated. Since TB1 did not significantly change the level of total mitochondrial proteins, TB1 may increase the turnover rate. In order to test this hypothesis, we used Mitotimer transgenic mice<sup>24</sup>, in which the turnover of mitochondria is conveniently monitored. Mitotimer marks old mitochondria with red, whereas new mitochondria appear green. HFD consumption increased the ratio of red to green, indicating that the proportion of old mitochondria was increased due to insufficient turnover (online Figure X A and B). After injection of TB1, however, the ratio of red to green was normalized (online Figure X A and B). Together with the fact that TB1 increases mitophagy, these results suggest that mitochondrial biogenesis and turnover are increased in response to TB1, even in the presence of HFD consumption. We performed EM analyses of the mitochondrial cristae structure<sup>25</sup>. HFD consumption increased the number of mitochondria with disconnected cristae. However, injection of TB1 attenuated this phenotype during HFD consumption (online Figure X C and D). The mitochondrial number did not change significantly (online Figure X E). Taken together, these results suggest that TB1 treatment attenuates mitochondrial dysfunction during the development of diabetic cardiomyopathy by increasing mitochondrial turnover.

## DISCUSSION

The early stage of diabetic cardiomyopathy includes the development of hypertrophy, intracellular lipid accumulation, fibrosis and diastolic dysfunction, which then evolves to



systolic dysfunction with reduced ejection fraction<sup>3,4</sup>. Our study suggests that HFD induces Atg7-dependent mitophagy in the early phase, which is partially mediated by a Parkin-dependent mechanism. Mitophagy serves as an essential quality control mechanism to maintain the function of mitochondria in the heart during HFD consumption. The impairment of mitophagy induces mitochondrial dysfunction and lipid accumulation, thereby exacerbating the development of diabetic cardiomyopathy.

Our results suggest that mitophagy is time-dependently activated in the heart in response to HFD feeding, as evidenced by increases in acidic dots of Mito-Keima and concomitant decreases in mtDNA consistent with increases in mitochondrial degradation. Furthermore, HFD increases localization of LC3II in the mitochondrial fraction, and the level of LC3II is further increased in the presence of CQ treatment, suggesting that autophagic flux of mitochondrial protein is increased in response to HFD. Much of the GFP-LC3 showed a ring-like structure and encircled mitochondria. Although increasing lines of evidence suggest that mitophagy can be mediated by both LC3-dependent and -independent autophagy, these results suggest that LC3-dependent autophagy mediates mitophagy in the heart during HFD consumption.

We found that general autophagy, evaluated with LC3II in the whole cell fraction, is activated by HFD feeding, peaking at 6 weeks, but declines thereafter. Interestingly, both LC3II in the mitochondrial fraction and mitophagy, evaluated with Mito-Keima, were increased even thereafter. It is possible that the activities of autophagy in the whole cell fraction and in mitochondria are differentially regulated. Interestingly, LC3II is observed predominantly in the mitochondrial fraction and the majority (>75%) of GFP-LC3 ring-like structures co-localized with mitochondria. Thus, activation of autophagy may take place primarily at mitochondria during HFD consumption, but the assessment of autophagy in the whole cell fraction may obscure its activation in mitochondria. Alternatively, additional mechanisms of mitophagy, such as LC3-independent mitophagy, may be activated after conventional mechanisms of autophagy are inactivated. We have shown previously that mitophagy is activated after general autophagy is inactivated during pressure overload<sup>9</sup>.

Mitophagy in response to HFD consumption is significantly attenuated in the presence of Atg7- or Parkin-downregulation, suggesting that Atg7- or Parkin-dependent mitophagy mediated through the conventional mechanism of autophagy is activated in the heart during HFD consumption. Importantly, acidic dots of Mito-Keima induced by HFD cannot be fully suppressed even in the presence of complete downregulation of Atg7 or Parkin, suggesting that either Atg7- or Parkin-independent mechanisms of mitophagy may also exist.

The development of cardiac hypertrophy, diastolic dysfunction, and cardiac fibrosis, typical features of diabetic cardiomyopathy in response to HFD feeding is exacerbated in *atg7*-cKO mice. These results suggest that Atg7-dependent activation of autophagy/mitophagy acts as an adaptive mechanism to protect the heart against diabetic cardiomyopathy. Because the majority of GFP-LC3 co-localized with mitochondria in control mice fed with HFD, we speculate that the suppressive effect of *atg7* cKO upon mitophagy is important. This notion is also supported by the fact that the cardiac phenotype observed in *atg7* cKO mice during HFD feeding is partially mimicked by that in Parkin KO mice.

One important consequence of mitophagy suppression is the development of mitochondrial dysfunction, including mitochondrial depolarization, reduced oxygen consumption and decreases in fatty acid oxidation. This leads to reduced ATP production and decreases in CM contraction. Indeed, systolic dysfunction develops in *atg7*cKO mice. It should be noted that systolic dysfunction was not observed in Parkin KO mice fed with HFD. One possibility is that Parkin-independent mechanisms of mitophagy remain in Parkin KO mice and contribute to the maintenance of mitochondrial function and cardiac contractility. Alternatively, downregulation of *Atg7* may more generally inactivate autophagy than that of Parkin. Consistently, TB1 increases mitophagy in Parkin KO mice. It should be noted that, regardless of Parkin-dependency, activation of mitophagy is effective in improving mitochondrial function and diastolic dysfunction in the heart in the presence of HFD consumption. Although we show that TB1 primarily increases LC3II in the mitochondrial fraction, suggesting that TB1 promotes mitophagy, we cannot formally exclude the possibility that increases in general autophagy may also contribute to the protective effect of TB1 during HFD consumption.

Increasing lines of evidence suggest that Parkin has multiple functions<sup>26</sup>. For example, Parkin stabilizes CD36 in the liver, whereas downregulation of Parkin decreases total body weight after five weeks of HFD feeding. Our results showed that body weight is increased after 2 months of HFD feeding and CD36 was not affected in the heart tissue of Parkin KO mice (online Figure VI). It is possible that the function of Parkin during HFD consumption may be time- and tissue-dependent.

Another important consequence of mitochondrial suppression is decreased fatty acid oxidation. If the level of fatty acid uptake is maintained, this can lead to accumulation of fatty acids in cells. In fact, we observed that LDs were larger and the level of Oil red O staining was enhanced in *atg7*cKO and Parkin KO mice. The greater extent of lipid accumulation in *atg7*cKO mice than in Parkin KO mice may be due to the fact that mitophagy is more extensively suppressed in *atg7*cKO mice than in Parkin KO mice. Accumulation of toxic fatty acids, such as ceramide and diacylglycerol, may induce deleterious effects, termed lipotoxicity. Since the formation of LDs alone is not necessarily toxic in some conditions<sup>27,28</sup>, whether lipid accumulation caused by suppression of mitophagy alone causes lipotoxicity remains to be elucidated.

It has been shown that lipophagy, selective autophagy that transfers lipid from LD to lysosome, assists lipolysis in liver cells and that lipophagy is ubiquitously observed<sup>29,30</sup>. Despite extensive search with EM, however, we were unable to identify autophagosomes containing LDs in adult CMs. In addition, we could not identify co-localization of GFP-LC3 and lipid in adult CMs freshly isolated from the heart of mice subjected to HFD feeding. Thus, we believe that autophagosomes sequester mitochondria rather than lipid in the heart in response to HFD consumption. Since lipophagy is believed to be a mechanism to facilitate lipolysis<sup>29</sup>, it is possible that it is not significantly activated under baseline conditions in the heart subjected to HFD feeding alone. We found that LDs observed in the heart after HFD feeding are almost all directly connected to mitochondria. The direct communication between mitochondria and LDs has been reported in previous studies<sup>31,32</sup>. Thus, it is likely that fatty acids are directly transferred from LDs to mitochondria in CMs under baseline

conditions or during HFD consumption. However, we cannot formally exclude the possibility that suppression of lipophagy contributes to the enhancement of lipid accumulation in *atg7* cKO mice. Further investigation is needed regarding the role of lipophagy in mediating fatty acid metabolism in the heart.

Since patients with insulin resistance frequently develop cardiac complications<sup>2</sup>, interventions to alleviate the cardiac effects of HFD consumption may lead to the development of a novel treatment for diabetic patients. Our results suggest that TAT-Beclin1 treatment is effective in preventing cardiac hypertrophy, diastolic dysfunction, and lipid accumulation in the hearts of mice subjected to HFD feeding, as well as enhancing mitophagy and mitochondrial biogenesis (Online Figure XI). Thus, treatment to increase mitophagy may be a promising modality to reduce cardiac complications in diabetic patients.

## Supplementary Material

Refer to Web version on PubMed Central for supplementary material.

## ACKNOWLEDGEMENTS

The authors thank Dr. Masaaki Komatsu (Tokyo Metropolitan Institute of Medical Science, Tokyo) for *atg7* flox/flox mice and Daniela Zablocki for critical reading of the manuscript.

### SOURCES OF FUNDING

This work was supported in part by U.S. Public Health Service Grants HL67724, HL91469, HL112330, HL138720 and AG23039 (J.S.) and by the Fondation Leducq Transatlantic Network of Excellence 15CBD04 (J.S.).

## Nonstandard Abbreviations and Acronyms:

<b><i>atg7</i> cKO</b>	cardiac-specific <i>atg7</i> knockout mice
<b>CM</b>	cardiomyocyte
<b>CQ</b>	chloroquine
<b>EDPVR</b>	end diastolic pressure-volume relationship
<b>EF</b>	ejection fraction
<b>EM</b>	electron microscopy
<b>ESPVR</b>	end systolic pressure-volume relationship
<b>FS</b>	fractional shortening
<b>HFD</b>	high fat diet
<b>LD</b>	lipid droplet
<b>LV</b>	left ventricular
<b>MMP</b>	mitochondrial membrane potential

<b>ND</b>	normal diet
<b>PV-Loop</b>	pressure volume loop
<b>TB1</b>	Tat-Beclin1
<b>TS1</b>	Tat-scramble
<b>Tg-GFP-LC3 mice</b>	transgenic mice expressing LC3 conjugated with green fluorescent protein
<b>Tg-Mito-Keima mice</b>	transgenic mice expressing Keima protein with a mitochondrial targeting sequence
<b>Tf-LC3 mice</b>	mRFP-GFP tandem fluorescent-tagged LC3 transgenic mice
<b>TMRE</b>	Tetramethylrhodamine ethyl ester, perchlorate

## REFERENCES

1. Afshin A, Forouzanfar MH, Reitsma MB, Sur P, Estep K, Lee A, Marczak L, Mokdad AH, Moradi-Lakeh M, Naghavi M, Salama JS, Vos T, Abate KH, Abbafati C, Ahmed MB, Al-Aly Z, Alkerwi A, Al-Raddadi R, Amare AT, Amberbir A, Amegah AK, Amini E, Amrock SM, Anjana RM, Arnlov J, Asayesh H, Banerjee A, Barac A, Baye E, Bennett DA, Beyene AS, Biadgilign S, Biryukov S, Bjertness E, Boneya DJ, Campos-Nonato I, Carrero JJ, Cecilio P, Cercy K, Ciobanu LG, Cornaby L, Damtew SA, Dandona L, Dandona R, Dharmaratne SD, Duncan BB, Eshrati B, Esteghamati A, Feigin VL, Fernandes JC, Furst T, Gebrehiwot TT, Gold A, Gona PN, Goto A, Habtewold TD, Hadush KT, Hafezi-Nejad N, Hay SI, Horino M, Islami F, Kamal R, Kasaeian A, Katikireddi SV, Kengne AP, Kesavachandran CN, Khader YS, Khang YH, Khubchandani J, Kim D, Kim YJ, Kinfu Y, Kosen S, Ku T, Defo BK, Kumar GA, Larson HJ, Leinsalu M, Liang X, Lim SS, Liu P, Lopez AD, Lozano R, Majeed A, Malekzadeh R, Malta DC, Mazidi M, McAlinden C, McGarvey ST, Mengistu DT, Mensah GA, Mensink GBM, Mezgebe HB, Mirrahimov EM, Mueller UO, Noubiap JJ, Obermeyer CM, Ogbo FA, Owolabi MO, Patton GC, Pourmalek F, Qorbani M, Rafay A, Rai RK, Ranabhat CL, Reinig N, Safiri S, Salomon JA, Sanabria JR, Santos IS, Sartorius B, Sawhney M, Schmidhuber J, Schutte AE, Schmidt MI, Sepanlou SG, Shamsizadeh M, Sheikhbahaei S, Shin MJ, Shiri R, Shiue I, Roba HS, Silva DAS, Silverberg JI, Singh JA, Stranges S, Swaminathan S, Tabares-Seisdedos R, Tadese F, Tedla BA, Tegegne BS, Terkawi AS, Thakur JS, Tonelli M, Topor-Madry R, Tyrovolas S, Ukwaja KN, Uthman OA, Vaezghasemi M, Vasankari T, Vlassov VV, Vollset SE, Weiderpass E, Werdecker A, Wesana J, Westerman R, Yano Y, Yonemoto N, Yonga G, Zaidi Z, Zenebe ZM, Zipkin B and Murray CJL. Health Effects of Overweight and Obesity in 195 Countries over 25 Years. *The New England journal of medicine*. 2017;377:13–27. [PubMed: 28604169]
2. Jia G, Hill MA and Sowers JR. Diabetic Cardiomyopathy: An Update of Mechanisms Contributing to This Clinical Entity. *Circulation research*. 2018;122:624–638. [PubMed: 29449364]
3. Yancy CW, Jessup M, Bozkurt B, Butler J, Casey DE Jr., Drazner MH, Fonarow GC, Geraci SA, Horwich T, Januzzi JL, Johnson MR, Kasper EK, Levy WC, Masoudi FA, McBride PE, McMurray JJ, Mitchell JE, Peterson PN, Riegel B, Sam F, Stevenson LW, Tang WH, Tsai EJ and Wilkoff BL. 2013 ACCF/AHA guideline for the management of heart failure: a report of the American College of Cardiology Foundation/American Heart Association Task Force on Practice Guidelines. *Journal of the American College of Cardiology*. 2013;62:e147–239. [PubMed: 23747642]
4. Yancy CW, Jessup M, Bozkurt B, Butler J, Casey DE Jr., Colvin MM, Drazner MH, Filippatos GS, Fonarow GC, Givertz MM, Hollenberg SM, Lindenfeld J, Masoudi FA, McBride PE, Peterson PN, Stevenson LW and Westlake C. 2017 ACC/AHA/HFSA Focused Update of the 2013 ACCF/AHA Guideline for the Management of Heart Failure: A Report of the American College of Cardiology/

- American Heart Association Task Force on Clinical Practice Guidelines and the Heart Failure Society of America. *Circulation*. 2017;136:e137–e161. [PubMed: 28455343]
5. Tong M and Sadoshima J. Mitochondrial autophagy in cardiomyopathy. *Current opinion in genetics & development*. 2016;38:8–15. [PubMed: 27003723]
  6. Kim JA, Wei Y and Sowers JR. Role of mitochondrial dysfunction in insulin resistance. *Circulation research*. 2008;102:401–14. [PubMed: 18309108]
  7. Drosatos K and Schulze PC. Cardiac lipotoxicity: molecular pathways and therapeutic implications. *Current heart failure reports*. 2013;10:109–21. [PubMed: 23508767]
  8. Ikeda Y, Shirakabe A, Maejima Y, Zhai P, Sciarretta S, Toli J, Nomura M, Mihara K, Egashira K, Ohishi M, Abdellatif M and Sadoshima J. Endogenous Drp1 mediates mitochondrial autophagy and protects the heart against energy stress. *Circ Res*. 2015;116:264–78. [PubMed: 25332205]
  9. Shirakabe A, Zhai P, Ikeda Y, Saito T, Maejima Y, Hsu CP, Nomura M, Egashira K, Levine B and Sadoshima J. Drp1-Dependent Mitochondrial Autophagy Plays a Protective Role Against Pressure Overload-Induced Mitochondrial Dysfunction and Heart Failure. *Circulation*. 2016;133:1249–63. [PubMed: 26915633]
  10. Sciarretta S, Maejima Y, Zablocki D and Sadoshima J. The Role of Autophagy in the Heart. *Annual review of physiology*. 2018;80:1–26.
  11. Xie Z, Lau K, Eby B, Lozano P, He C, Pennington B, Li H, Rathi S, Dong Y, Tian R, Kem D and Zou MH. Improvement of cardiac functions by chronic metformin treatment is associated with enhanced cardiac autophagy in diabetic OVE26 mice. *Diabetes*. 2011;60:1770–8. [PubMed: 21562078]
  12. Sciarretta S, Zhai P, Shao D, Maejima Y, Robbins J, Volpe M, Condorelli G and Sadoshima J. Rheb is a critical regulator of autophagy during myocardial ischemia: pathophysiological implications in obesity and metabolic syndrome. *Circulation*. 2012;125:1134–46. [PubMed: 22294621]
  13. Xu X, Kobayashi S, Chen K, Timm D, Volden P, Huang Y, Gulick J, Yue Z, Robbins J, Epstein PN and Liang Q. Diminished autophagy limits cardiac injury in mouse models of type 1 diabetes. *J Biol Chem*. 2013;288:18077–92. [PubMed: 23658055]
  14. Kanamori H, Takemura G, Goto K, Tsujimoto A, Mikami A, Ogino A, Watanabe T, Morishita K, Okada H, Kawasaki M, Seishima M and Minatoguchi S. Autophagic adaptations in diabetic cardiomyopathy differ between type 1 and type 2 diabetes. *Autophagy*. 2015;11:1146–60. [PubMed: 26042865]
  15. Jaishy B, Zhang Q, Chung HS, Riehle C, Soto J, Jenkins S, Abel P, Cowart LA, Van Eyk JE and Abel ED. Lipid-induced NOX2 activation inhibits autophagic flux by impairing lysosomal enzyme activity. *Journal of lipid research*. 2015;56:546–61. [PubMed: 25529920]
  16. Mellor KM, Bell JR, Young MJ, Ritchie RH and Delbridge LM. Myocardial autophagy activation and suppressed survival signaling is associated with insulin resistance in fructose-fed mice. *Journal of molecular and cellular cardiology*. 2011;50:1035–43. [PubMed: 21385586]
  17. Russo SB, Baicu CF, Van Laer A, Geng T, Kasiganesan H, Zile MR and Cowart LA. Ceramide synthase 5 mediates lipid-induced autophagy and hypertrophy in cardiomyocytes. *The Journal of clinical investigation*. 2012;122:3919–30. [PubMed: 23023704]
  18. Hariharan N, Zhai P and Sadoshima J. Oxidative stress stimulates autophagic flux during ischemia/reperfusion. *Antioxid Redox Signal*. 2011;14:2179–90. [PubMed: 20812860]
  19. Eisenberg T, Abdellatif M, Schroeder S, Primessnig U, Stekovic S, Pendl T, Harger A, Schipke J, Zimmermann A, Schmidt A, Tong M, Ruckstuhl C, Dammbroeck C, Gross AS, Herbst V, Magnes C, Trausinger G, Narath S, Meinitzer A, Hu Z, Kirsch A, Eller K, Carmona-Gutierrez D, Buttner S, Pietrocola F, Knittelfelder O, Schrepfer E, Rockenfeller P, Simonini C, Rahn A, Horsch M, Moreth K, Beckers J, Fuchs H, Gailus-Durner V, Neff F, Janik D, Rathkolb B, Rozman J, de Angelis MH, Moustafa T, Haemmerle G, Mayr M, Willeit P, von Frieling-Salewsky M, Pieske B, Scorrano L, Pieber T, Pechlaner R, Willeit J, Sigrist SJ, Linke WA, Muhlfeld C, Sadoshima J, Dengel J, Kiechl S, Kroemer G, Sedej S and Madeo F. Cardioprotection and lifespan extension by the natural polyamine spermidine. *Nat Med*. 2016;22:1428–1438. [PubMed: 27841876]
  20. Maejima Y, Kyoj S, Zhai P, Liu T, Li H, Ivessa A, Sciarretta S, Del Re DP, Zablocki DK, Hsu CP, Lim DS, Isobe M and Sadoshima J. Mst1 inhibits autophagy by promoting the interaction between Beclin1 and Bcl-2. *Nature medicine*. 2013;19:1478–88.

21. Shirakabe A, Fritzky L, Saito T, Zhai P, Miyamoto S, Gustafsson AB, Kitsis RN and Sadoshima J. Evaluating mitochondrial autophagy in the mouse heart. *J Mol Cell Cardiol.* 2016;92:134–9. [PubMed: 26868976]
22. Cingolani F and Czaja MJ. Regulation and Functions of Autophagic Lipolysis. *Trends in endocrinology and metabolism: TEM.* 2016;27:696–705. [PubMed: 27365163]
23. Shoji-Kawata S, Sumpter R, Leveno M, Campbell GR, Zou Z, Kinch L, Wilkins AD, Sun Q, Pallauf K, MacDuff D, Huerta C, Virgin HW, Helms JB, Eerland R, Tooze SA, Xavier R, Lenschow DJ, Yamamoto A, King D, Lichtarge O, Grishin NV, Spector SA, Kaloyanova DV and Levine B. Identification of a candidate therapeutic autophagy-inducing peptide. *Nature.* 2013;494:201–6. [PubMed: 23364696]
24. Laker RC, Xu P, Ryall KA, Sujkowski A, Kenwood BM, Chain KH, Zhang M, Royal MA, Hoehn KL, Driscoll M, Adler PN, Wessells RJ, Saucerman JJ and Yan Z. A novel MitoTimer reporter gene for mitochondrial content, structure, stress, and damage in vivo. *The Journal of biological chemistry.* 2014;289:12005–15. [PubMed: 24644293]
25. Cogliati S, Frezza C, Soriano ME, Varanita T, Quintana-Cabrera R, Corrado M, Cipolat S, Costa V, Casarin A, Gomes LC, Perales-Clemente E, Salviati L, Fernandez-Silva P, Enriquez JA and Scorrano L. Mitochondrial cristae shape determines respiratory chain supercomplexes assembly and respiratory efficiency. *Cell.* 2013;155:160–71. [PubMed: 24055366]
26. Shires SE, Kitsis RN and Gustafsson AB. Beyond Mitophagy: The Diversity and Complexity of Parkin Function. *Circulation research.* 2017;120:1234–1236. [PubMed: 28408450]
27. Sinha RA, Singh BK, Zhou J, Xie S, Farah BL, Lesmana R, Ohba K, Tripathi M, Ghosh S, Hollenberg AN and Yen PM. Loss of ULK1 increases RPS6KB1-NCOR1 repression of NR1H/ LXR-mediated Scd1 transcription and augments lipotoxicity in hepatic cells. *Autophagy.* 2017;13:169–186. [PubMed: 27846372]
28. Lee SJ, Zhang J, Choi AM and Kim HP. Mitochondrial dysfunction induces formation of lipid droplets as a generalized response to stress. *Oxidative medicine and cellular longevity.* 2013;2013:327167. [PubMed: 24175011]
29. Martinez-Lopez N and Singh R. Autophagy and Lipid Droplets in the Liver. *Annual review of nutrition.* 2015;35:215–37.
30. Singh R and Cuervo AM. Lipophagy: connecting autophagy and lipid metabolism. *International journal of cell biology.* 2012;2012:282041. [PubMed: 22536247]
31. Aon MA, Bhatt N and Cortassa SC. Mitochondrial and cellular mechanisms for managing lipid excess. *Frontiers in physiology.* 2014;5:282. [PubMed: 25132820]
32. Wang H, Sreenivasan U, Hu H, Saladino A, Polster BM, Lund LM, Gong DW, Stanley WC and Sztalryd C. Perilipin 5, a lipid droplet-associated protein, provides physical and metabolic linkage to mitochondria. *Journal of lipid research.* 2011;52:2159–68. [PubMed: 21885430]



## NOVELTY AND SIGNIFICANCE

### What Is Known?

- Diabetic cardiomyopathy is often accompanied by mitochondrial dysfunction.
- Autophagy is either upregulated or downregulated in the heart during high fat diet consumption.
- Diabetic cardiomyopathy is characterized by intramyocardial lipid accumulation, termed lipotoxicity.

### What New Information Does This Article Contribute?

- Mitophagy is activated but insufficient for the maintenance of mitochondrial function during the initial phase of diabetic cardiomyopathy.
- Atg7-dependent mitophagy maintains mitochondrial function and protects against hypertrophy and diastolic dysfunction during the initial phase of diabetic cardiomyopathy.
- Stimulation of mitophagy by TAT-Beclin 1 inhibits the development of diabetic cardiomyopathy.
- Suppression of mitophagy increases accumulation of lipids in the heart during high fat diet consumption.

Diabetic patients commonly develop cardiac dysfunction characterized by hypertrophy and diastolic dysfunction, termed diabetic cardiomyopathy. Intramyocardial lipid accumulation and mitochondrial dysfunction are intimately involved in the pathogenesis of diabetic cardiomyopathy. We found that autophagy primarily targeting mitochondria, namely mitophagy, is activated during the early phase of high fat diet (HFD) consumption in a mouse model of type II diabetes. Mitophagy activated during the early phase of HFD consumption is both Atg7- and Parkin-dependent. Suppression of mitophagy through downregulation of either Atg7 or Parkin exacerbated mitochondrial dysfunction and cardiac dysfunction during HFD consumption. Thus, although mitophagy is activated during the early development of diabetic cardiomyopathy, it is insufficient to protect the heart. Enhancement of mitophagy by TAT-Beclin 1 improved mitochondrial function by enhancing mitochondrial turnover and reducing lipid accumulation in the heart, thereby alleviating the development of diabetic cardiomyopathy. These results suggest that Atg7- and Parkin-dependent mitophagy plays an essential role in the maintenance of mitochondrial function and protects the heart during the early development of diabetic cardiomyopathy.

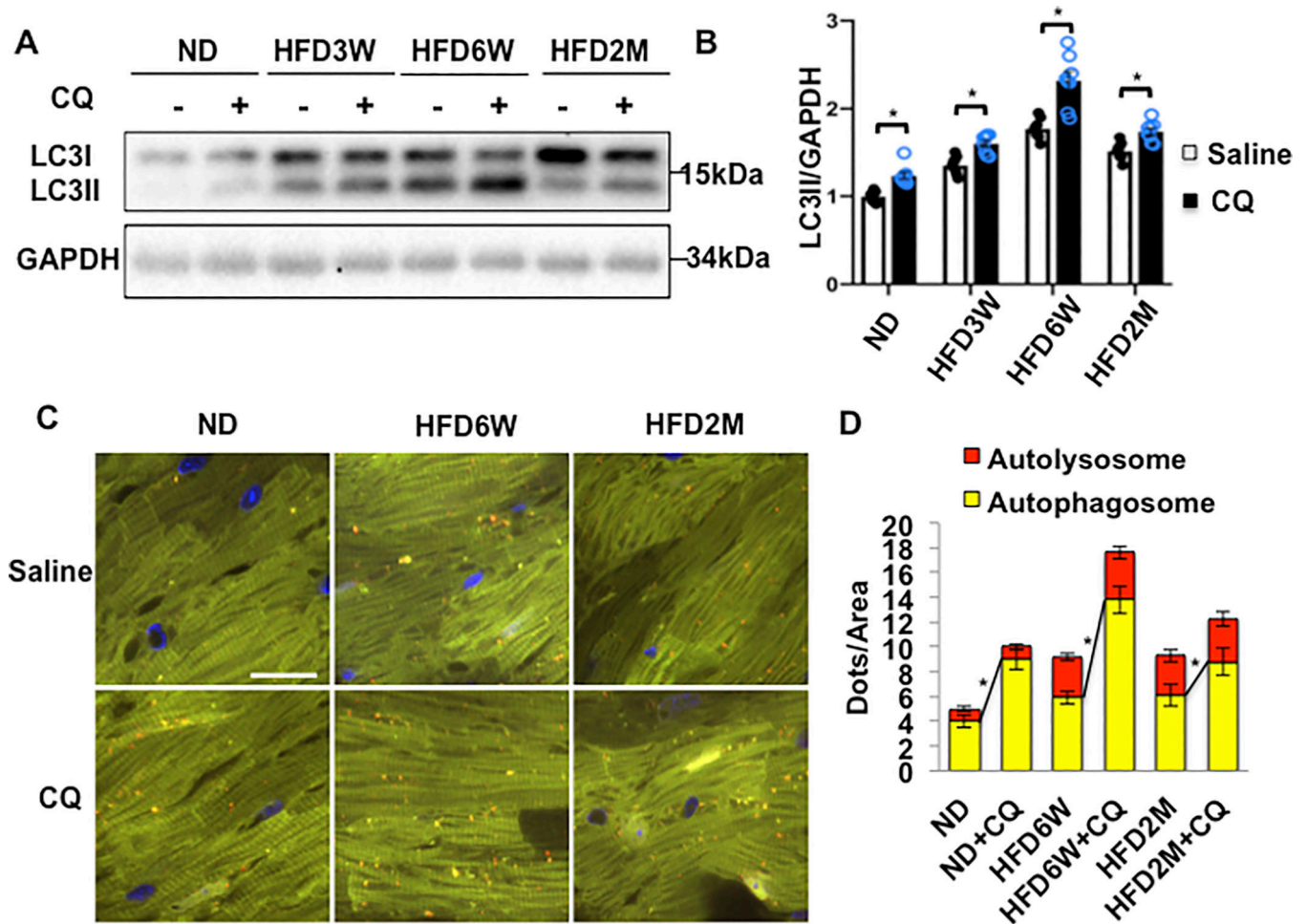


**Figure 1. Autophagic flux in the heart was increased after 6 weeks of HFD feeding but inhibited after 2 months of HFD feeding.**

(A) Evaluation of autophagic flux by Western blotting of LC3II protein. (B) Quantification of LC3II at different time points (n=8 in each group. Values are means  $\pm$  S.E. \*,  $p < 0.05$  using unpaired Student *t* test). (C) Evaluation of autophagic flux with TF-LC3 mice. (D) Quantification of autolysosome (red) and autophagosome (yellow) dots (n=8 in each group. Values are means  $\pm$  S.E. \*,  $p < 0.05$  using unpaired Student *t* test). Scale bar = 100  $\mu$ m.

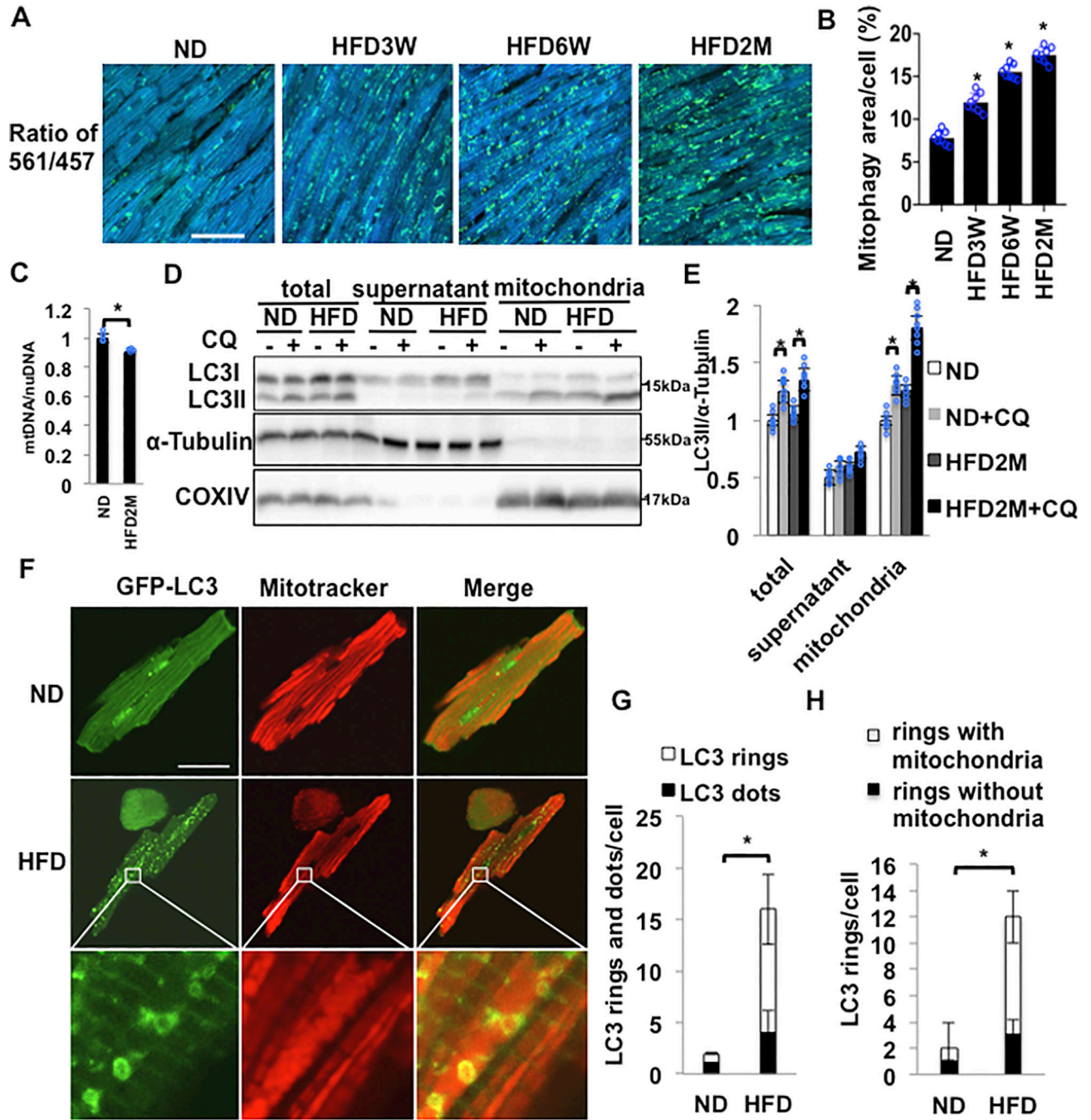


**Figure 2. Mitophagy in the heart was upregulated in response to HFD feeding.** (A) Evaluation of mitophagy in cardiac specific Mito-Kiema transgenic mice fed ND or HFD for different durations. Areas with 561/457 nm ratios, indicating mitophagy, are shown. Scale bar = 50µm. (B) Quantification of the mitophagy area at different time points (n=8 in each group. Values are means ± S.E. \*, p<0.05 using unpaired Student *t* test). (C) Relative mitochondrial DNA content normalized by nuclear DNA content was decreased after 2 months of HFD feeding (n=4 in each group. Values are means ± S.E. \*, p<0.05 using unpaired Student *t* test). (D,E) Representative immunoblots and quantitative analyses of

whole-cell heart homogenates and isolated mitochondria for LC3II,  $\alpha$ -Tubulin and COXIV. Whole-cell heart homogenates, the mitochondrial fraction, and the supernatant fraction were prepared from mice subjected to either ND or HFD feeding for 2 months. (n=8 in each group. Values are means  $\pm$  S.E. \*, p<0.05 using unpaired Student *t* test). (F-H) Representative fluorescent images and quantitative analyses of adult CMs isolated from cardiac Tg-GFP-LC3 mice subjected to either ND or 2 months of HFD feeding. CMs were incubated with Mitotracker. HFD increased either GFP-LC3 dots or GFP-LC3 rings. Many GFP-LC3 rings were enriched with mitochondria (n=8 in each group. The number of CMs is 50 in each group. Values are means  $\pm$  S.E. \*, p<0.05 using unpaired Student *t* test). Scale bar = 50  $\mu$ m.



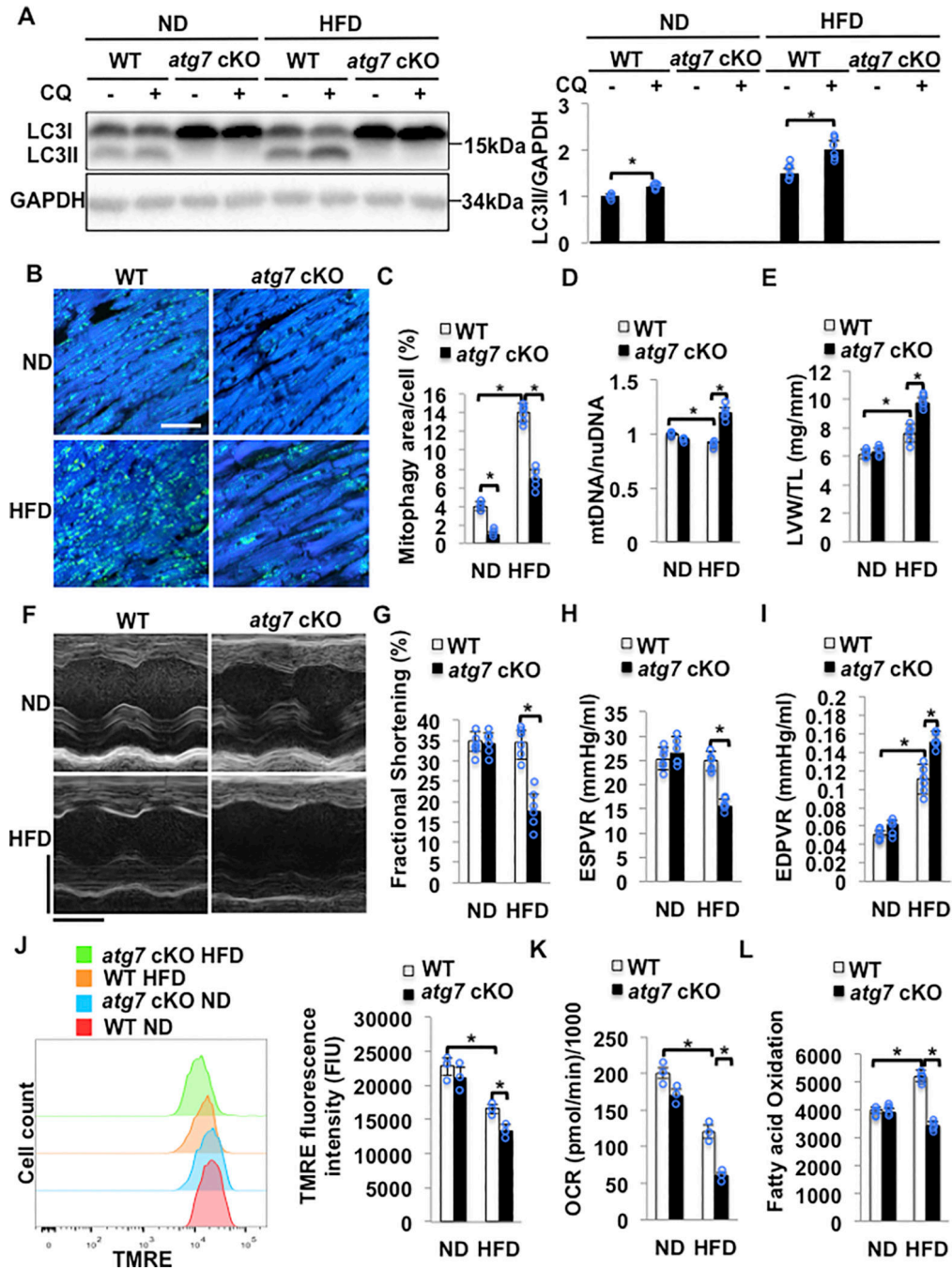


**Figure 3. HFD feeding induced cardiac dysfunction in *atg7* cKO mice.** WT and *atg7* cKO mice were subjected to either ND or HFD feeding for 2 months.

(A) Representative immunoblots and quantitative analysis of whole-cell heart homogenates for LC3II in WT and *atg7* cKO mice. N=5–6 in each group. Values are means ± S.E. \*, p<0.05 using unpaired Student *t* test. (B,C) Representative fluorescent images and quantitative analyses of mitophagy in Tg-Mito-Keima mice crossed with WT or *atg7* cKO mice and fed with either ND or HFD. Scale bar = 50µm. N=5–6 in each group. Values are means ± S.E. \*, p<0.05 using one way ANOVA followed by Bonferroni's *post-hoc* test. (D) Relative mitochondrial DNA content/nuclear DNA content was greater in *atg7* cKO mice

with HFD than in WT mice with HFD. N=5–6 in each group. Values are means  $\pm$  S.E. \*,  $p < 0.05$  using one way ANOVA followed by Bonferroni's *post-hoc* test. (E) Quantitative analyses of LVW/TL. N=5–6 in each group. Values are means  $\pm$  S.E. \*,  $p < 0.05$  using one way ANOVA followed by Bonferroni's *post-hoc* test. (F). Representative M mode tracing of echocardiographs. Scale bars, horizontal 100 ms and vertical 2 mm. (G) Left ventricular fractional shortening (LVFS) was evaluated by echocardiography. N=5–6 in each group. Values are means  $\pm$  S.E. \*,  $p < 0.05$  using one way ANOVA followed by Bonferroni's *post-hoc* test. (H) ESPVR evaluated by PV-Loop analysis showed that *atg7* cKO mice developed severe cardiac systolic dysfunction following 2 months of HFD feeding. N=5–6 in each group. Values are means  $\pm$  S.E. \*,  $p < 0.05$  using one way ANOVA followed by Bonferroni's *post-hoc* test. (I) EDPVR evaluated by PV-Loop analysis showed that *atg7* cKO mice developed severe cardiac diastolic dysfunction following two months of HFD feeding. N=5–6 in each group. Values are means  $\pm$  S.E. \*,  $p < 0.05$  using one way ANOVA followed by Bonferroni's *post-hoc* test. (J) Representative results of flow cytometric analyses and quantitative analyses of TMRE intensity in adult CMs isolated from the indicated group, showing that the MMP was decreased in *atg7* cKO mice fed with HFD. N=3 in each group. Values are means  $\pm$  S.E. \*,  $p < 0.05$  using one way ANOVA followed by Bonferroni's *post-hoc* test. (K) Mitochondrial oxygen consumption rate (OCR) in isolated CMs was evaluated with Sea Horse Analyzer. N=3 in each group. Values are means  $\pm$  S.E. \*,  $p < 0.05$  using one way ANOVA followed by Bonferroni's *post-hoc* test. (L) Fatty acid oxidation was evaluated with [3H]-oleic acid. Increases in fatty acid oxidation in response to HFD feeding were abolished in *atg7* cKO mice. N=5 in each group. Values are means  $\pm$  S.E. \*,  $p < 0.05$  using one way ANOVA followed by Bonferroni's *post-hoc* test.



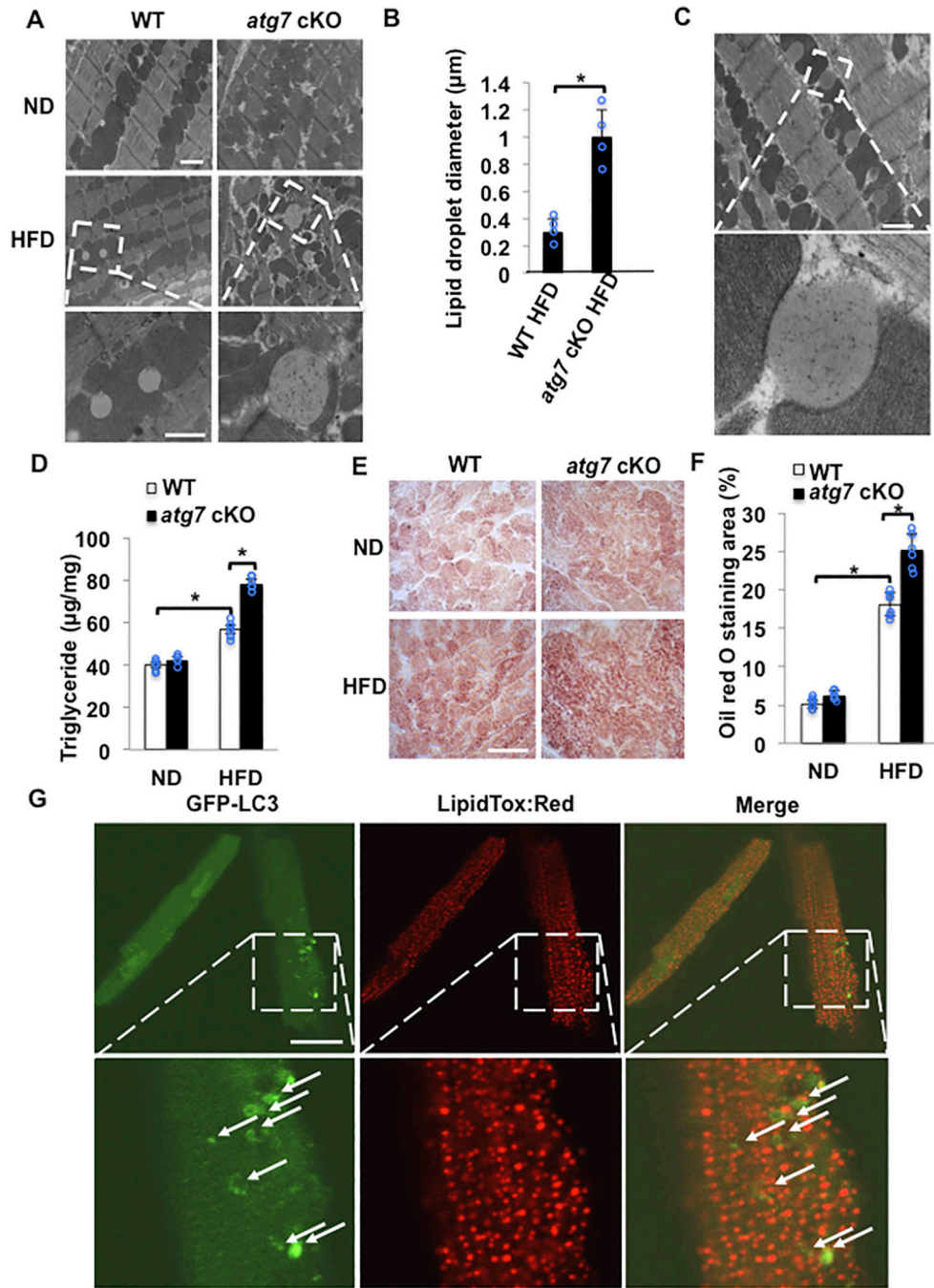


**Figure 4. Lipid accumulation in response to HFD feeding was enhanced in *atg7* cKO mice compared to in WT mice.** (A,B) Representative EM images and quantitative analyses of mouse hearts. The hearts of *atg7* cKO mice fed with HFD exhibited larger LDs. N=4 in each group. Values are means ± S.E. \*, p<0.05 using unpaired Student *t* test. Scale bar = 500nm. (C) EM images of LDs in a WT mouse heart fed with HFD. Scale bar = 500nm. (D) Quantitative analyses of triglyceride levels in the heart tissue. N=6 in each group. Values are means ± S.E. \*, p<0.05 using one way ANOVA followed by Bonferroni's *post-hoc* test. (E) Oil red O staining of cardiac tissues. Scale bar = 50 µm. (F) Quantification of Oil red O positive area. N=6 in each group.

Values are means  $\pm$  S.E. \*,  $p < 0.05$  using one way ANOVA followed by Bonferroni's *post-hoc* test. (G) CMs were isolated from Tg-GFP-LC3 mice fed with HFD for 2 months, and then stained with LipidTox red. Autophagosomes with double membrane containing lipid inside were not observed. The number of CMs is 50 in each group. Scale bar = 50  $\mu$ m.

Author Manuscript

Author Manuscript

Author Manuscript

Author Manuscript

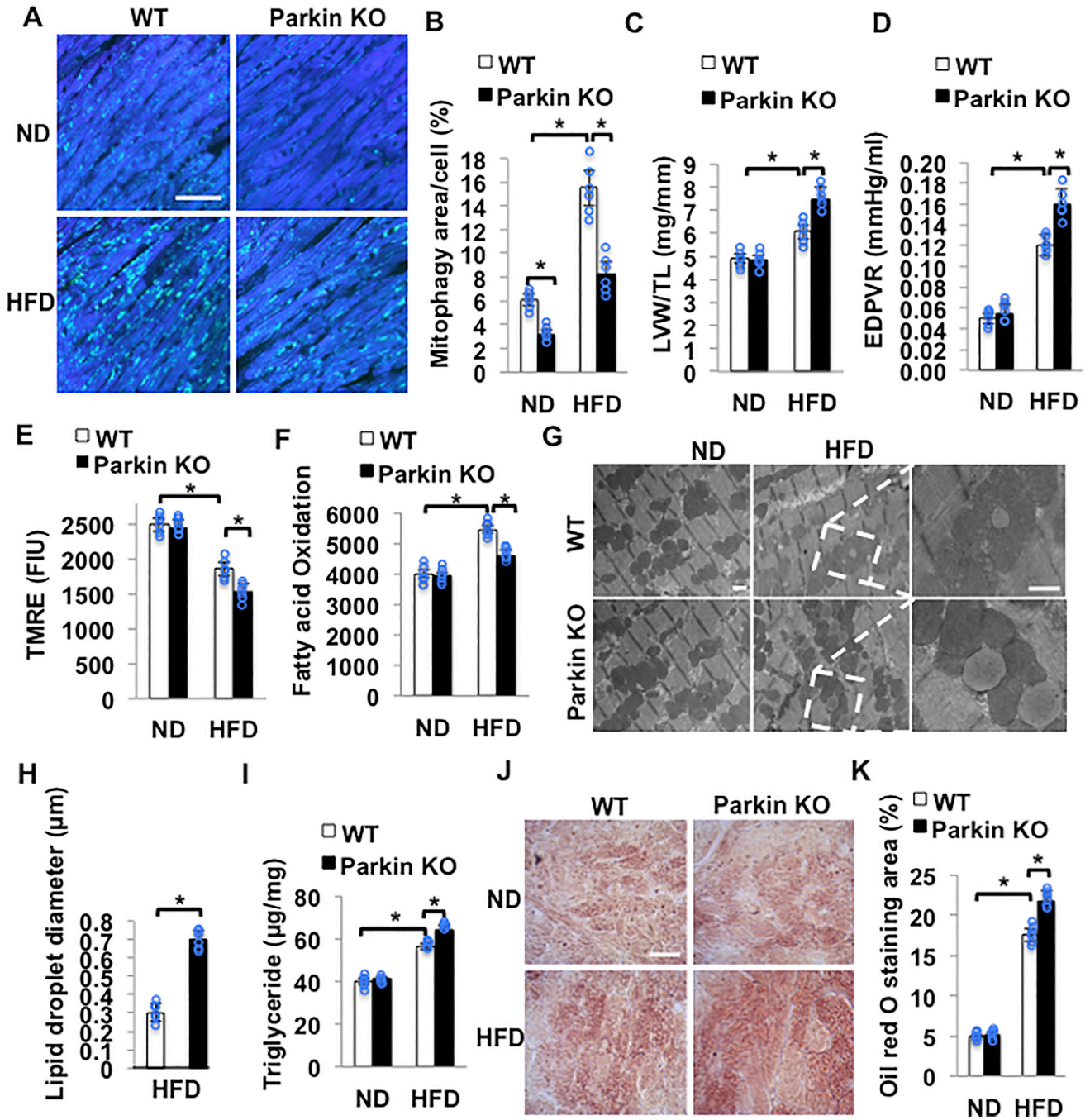


**Figure 5. HFD feeding induces cardiac dysfunction in Parkin KO mice. Parkin KO and WT mice were fed with ND or HFD for 2 months.**

(A,B) Representative fluorescent images and quantitative analyses of mitophagy. WT and Parkin KO mice were crossed with Tg-Mito-Keima mice and then fed with either ND or HFD. Scale bar = 50µm. N=6 in each group. Values are means ± S.E. \*, p<0.05 using one way ANOVA followed by Bonferroni's *post-hoc* test. (C) Quantitative analyses of LVW/TL. N=5–6 in each group. Values are means ± S.E. \*, p<0.05 using one way ANOVA followed by Bonferroni's *post-hoc* test. (D) EDPVR evaluated by PV-Loop analysis showed that Parkin KO mice developed severe cardiac diastolic dysfunction after 2 months of HFD

feeding. N=5–6 in each group. Values are means  $\pm$  S.E. \*,  $p < 0.05$  using one way ANOVA followed by Bonferroni's *post-hoc* test. (E) Quantitative analyses of TMRE intensity in freshly isolated adult CMs. Mitochondrial membrane potential was decreased in Parkin KO mice fed with HFD. N=6 in each group. Values are means  $\pm$  S.E. \*,  $p < 0.05$  using one way ANOVA followed by Bonferroni's *post-hoc* test. (F) Fatty acid oxidation was decreased in Parkin KO mice compared to in WT mice during HFD. N=6 in each group. Values are means  $\pm$  S.E. \*,  $p < 0.05$  using one way ANOVA followed by Bonferroni's *post-hoc* test. (G,H) Representative EM images and quantitative analyses of mouse hearts showed that larger LDs accumulated in Parkin KO mice fed with HFD. N=6 in each group. Values are means  $\pm$  S.E. \*,  $p < 0.05$  using unpaired Student *t* test. Scale bar = 500nm (I) Quantitative analyses of triglyceride levels in the heart tissue. N=6 in each group. Values are means  $\pm$  S.E. \*,  $p < 0.05$  using one way ANOVA followed by Bonferroni's *post-hoc* test. (J) Oil red O staining of cardiac tissues. Scale bar = 50  $\mu$ m (K) Quantification of Oil red O positive area. N=6 in each group. Values are means  $\pm$  S.E. \*,  $p < 0.05$  using one way ANOVA followed by Bonferroni's *post-hoc* test.



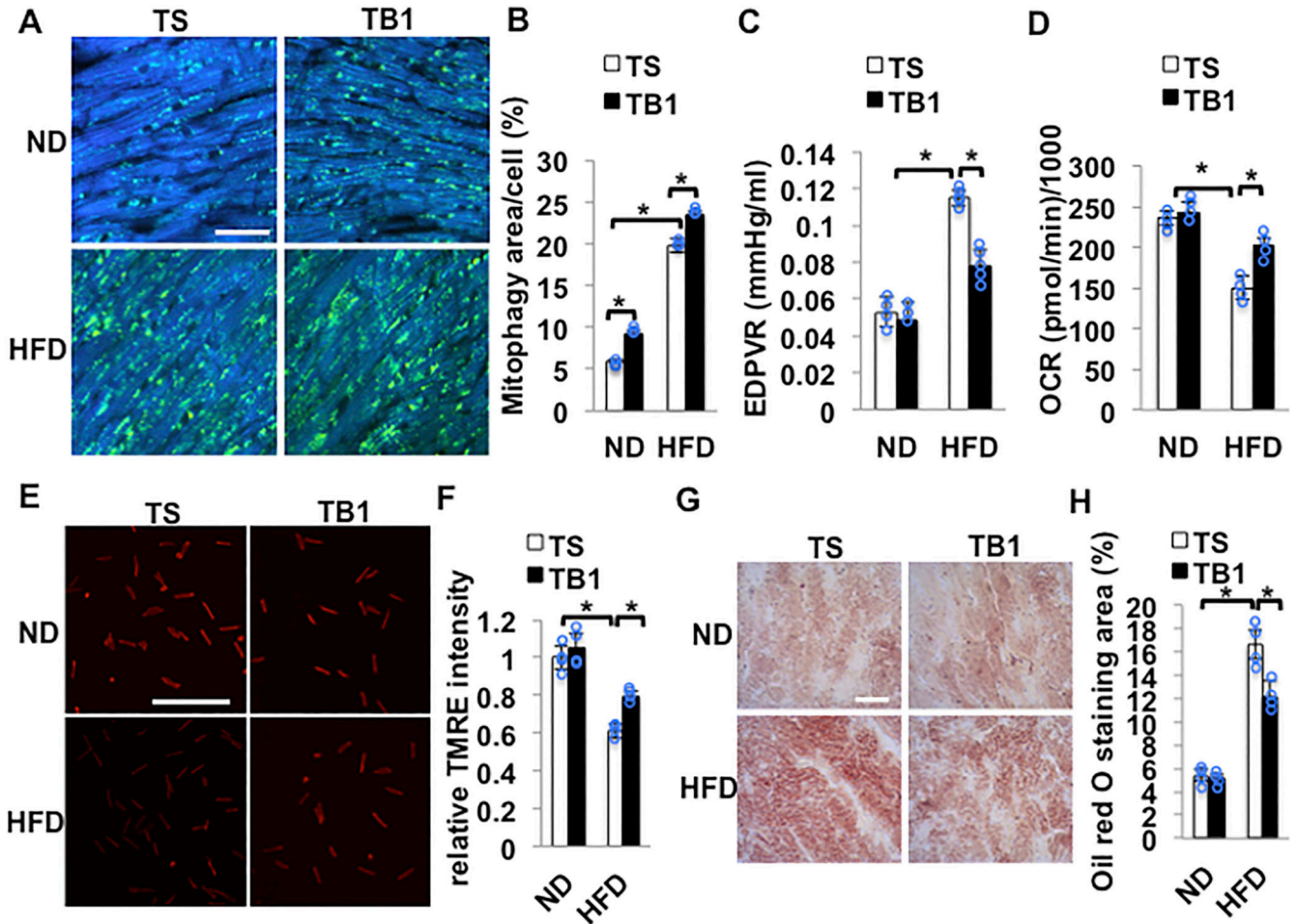


**Figure 6. HFD-induced cardiac dysfunction was attenuated by TB1.**

(A,B) Mitophagy was upregulated following injection of TB1. Tg-Mito-Keima mice were fed with ND or HFD for 3 months. Mice were injected intraperitoneally with TS or TB1 at 20 mg/kg daily for 2 weeks, beginning after 10 weeks of HFD feeding. Areas with high ratios (561/457) of Mito-Keima signals, indicating mitophagy, are shown. Representative fluorescent images and quantitative analysis of mitophagy. Scale bar = 50 $\mu$ m. N=4 in each group. Values are means  $\pm$  S.E. \*,  $p < 0.05$  using one way ANOVA followed by Bonferroni's *post-hoc* test. (C) EDPVR evaluated by PV-Loop analysis showed HFD-induced cardiac diastolic dysfunction was attenuated by injection of TB1 compared with TS. N=3–5 in each group. Values are means  $\pm$  S.E. \*,  $p < 0.05$  using one way ANOVA followed by Bonferroni's *post-hoc* test. (D) Mitochondrial oxygen consumption rate (OCR) from isolated CMs was evaluated with Sea Horse Analyzer. N=4 in each group. Values are means  $\pm$  S.E. \*,  $p < 0.05$  using one way ANOVA followed by Bonferroni's *post-hoc* test. (E,F) Quantitative analyses of TMRE intensity freshly isolated from adult CMs. Representative fluorescent images and quantitative analysis of TMRE staining indicated that mitochondrial membrane potential was preserved with injection of TB1. The number of CMs is 500 in each group. Values are means  $\pm$  S.E. \*,  $p < 0.05$  using one way ANOVA followed by Bonferroni's *post-hoc* test. Scale bar = 500 $\mu$ m. (G) Oil red O staining of cardiac tissues. Scale bar = 50 $\mu$ m. (H)

Quantification of Oil red O positive area. N=4 in each group. Values are means  $\pm$  S.E. \*, p<0.05 using one way ANOVA followed by Bonferroni's *post-hoc* test.

Author Manuscript

Author Manuscript

Author Manuscript

Author Manuscript